LAWRENCE
LIVERMORE
NATIONAL
LABORATORY

LLNL-AR-417502

2009 LLNL Nuclear Forensics Summer Program

Annie B. Kersting, Nancy A. Hutcheon

October 2, 2009

Disclaimer

This work performed under the auspices of the U.S. Department of Energy by Lawrence Livermore National Laboratory under Contract DE-AC52-07NA27344.

2009 LLNL Nuclear Forensics Summer Program

Lawrence Livermore National Laboratory
Physical and Life Sciences
Glenn T. Seaborg Institute
Livermore, CA 94550, USA

Director: Annie Kersting (kersting1@llnl.gov)
Education Coordinator: Nancy Hutcheon
Administrator: Camille Vandermeer
Web site https://seaborg.llnl.gov

Sponsors:
National Technical Nuclear Forensics Center, Domestic Nuclear Detection Office, Department of Homeland Security
LLNL: Glenn T. Seaborg Institute, Chemistry, Materials, Earth and Life Sciences Directorate

Glenn T. Seaborg Institute

The Lawrence Livermore National Laboratory (LLNL) Nuclear Forensics Summer Program is designed to give both undergraduate and graduate students an opportunity to come to LLNL for 8-10 weeks during the summer for a hands-on research experience. Students conduct research under the supervision of a staff scientist, attend a weekly lecture series, interact with other students, and present their work in poster format at the end of the program. Students also have the opportunity to participate in LLNL facility tours (e.g. National Ignition Facility, Center of Accelerator Mass-spectrometry) to gain a better understanding of the multi-disciplinary science that is on-going at LLNL.

Currently called the Nuclear Forensics Summer Program, this program began ten years ago as the Actinide Sciences Summer Program. The program is run within the Glenn T. Seaborg Institute in the Chemistry, Materials, Earth and Life Sciences Directorate at LLNL. The goal of Nuclear Forensics Summer Program is to facilitate the training of the next generation of nuclear scientists and engineers to solve critical national security problems in the field of nuclear forensics. We select students who are majoring in physics, chemistry, nuclear engineering, chemical engineering and environmental sciences. Students engage in research projects in the disciplines of actinide and radiochemistry, isotopic analysis, radiation detection, and nuclear engineering in order to strengthen the 'pipeline' for future scientific disciplines critical to DHS, NNSA.

This is a competitive program with over 200 applicants for the 8-10 slots available. Students come highly recommended from universities all over the country. For example, this year we hosted students from UC Davis, Cal State San Louis Obispo, Univ. of Nevada, Univ. of Wyoming, Northwestern, Univ. of New Mexico and Arizona State Univ. We advertise with mailers and email to physics, engineering, geochemistry and chemistry departments throughout the U.S. We also host students for a day at LLNL who are participating in the D.O.E. sponsored "*Summer School in Nuclear Chemistry"* course held at San Jose State University and have recruited from this program.

This year students conducted research on such diverse topics as: isotopic fingerprinting, statistical modeling in nuclear forensics, uranium analysis for nuclear forensics, environmental radiochemistry, analysis of nuclear test debris for nuclear forensics, trans-actinide nuclear chemistry, and actinide separations chemistry.

Graduate students are invited to return for a second year at their mentor's discretion. For the top graduate students in our program, we encourage the continuation of research collaboration between graduate student, faculty advisor and laboratory scientists. This creates a successful pipeline of top quality students from universities across the U.S. Since 2002, 20 summer students have continued to conduct their graduate research at LLNL, 7 have become postdoctoral fellows, and 7 have been hired as career scientists.

2009 Summer Students at Work

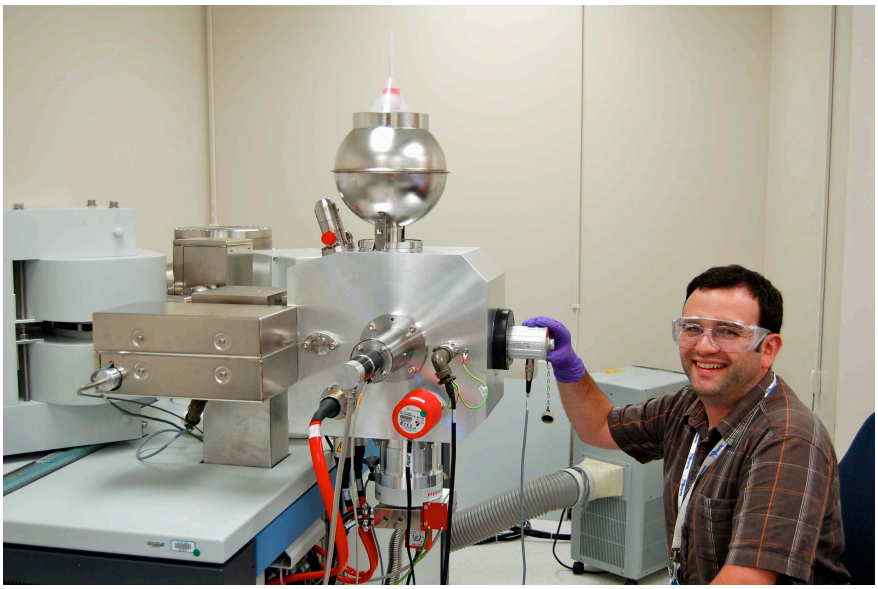

Summer Student Roster 2009

Student	Major	University	Year
Colleen Barton	Chemistry	Cal State San Louis Obispo	Undergrad
Megan Bennett	Radiochemistry	Univ. Nevada Las Vegas	Grad
Greg Brennecka	Geochemistry	Arizona State Univ.	Grad
Chris Cox	Geology	Univ. of Wyoming	Grad
Ben Jacobsen	Geochemistry	UC Davis	Grad
Jordan Klingsporn	Chemistry	Northwestern	Grad
Naomi Marks	Geochemistry	UC Davis	Grad
Chrystal Tulley	Chemistry/Water Resources	Univ. of New Mexico	Grad

Seminar Schedule 2009

Date	Speaker	Title of Presentation
June 24	Ken Moody, LLNL	Superheavy Element Research
July 1	Sarah Nelson, previous summer student LLNL postdoc	Novel Actinide Separations, Or - LLNL Undergrad to LLNL Postdoc: How Did I Do It?
July 1	Greg Brennecka, returning summer student: Arizona State University	Uranium Isotope Measurements in Nuclear Materials: Geo-Location of Uranium ore Concentrate.
July 1	Bret Isselhardt, previous summer student U.C. Berkeley grad. student	Uranium Isotope Ratios by Resonance Ionization Mass Spectrometry for a Nuclear Forensic Application
July 8	Jean Moran, Cal. State East Bay	Tracing Groundwater and Contaminants Using Isotopes
July 22	Adam Bernstein, LLNL	Detectors for Nuclear Forensics
July 27	Sig Hecker, Stanford, former Director of LANL	North Korea Revisited
July 29	Jay Davis, former director of DTRA	Preparing for the Experiment one Hopes Never to do
August 5	Poster Session	

Tracing nitrate through the unsaturated zone of dairies with sustainable conservation programs

Colleen Barton, Nuclear Forensics Internship Program (Cal Poly, San Luis Obispo)
Brad Esser, Sarah Roberts, Rachel Lindvall (CSD/PLS)

Glenn T. Seaborg Institute

Introduction

Nitrate is the major contaminants of groundwater in the United States. Sources of nitrate are fertilizers, septic systems and animal manure. The dairy industry is a major part of California agriculture and, it is important to know how these operations affect the environment. Groundwaters underlying large animal operations have unusually high amounts of nitrate, and recent legislation is requiring dairies to implement nutrient management plans. State funding through Sustainable Conservation have allowed several dairies to implement changes in nutrient and water management to reduce contamination of groundwater.

In the current study, three participating dairies in the San Joaquin Valley were studied by LLNL to assess the impact of management practice changes on groundwater quality. The general approach is to determine groundwater age in monitor wells and transit time through the vadose zone in order to determine when changes in dairy management will impact underlying groundwater quality. The two dairies shown here are in the southern Tulare Basin, and represent one of the youngest (36-04) and the oldest (36-19) dairies in the region.

Methods

Groundwater age is the mean time of transport from the water table to the monitor well screen, and has been determined for wells in this study using the tritium/helium-3 method. Groundwater age does not include transit of water and nitrate between the dairy farm ground surface through the vadose zone to the water table. In southern dairies, where depth to water varies between 50 and 150 feet, vadose zone transport time may be significant.

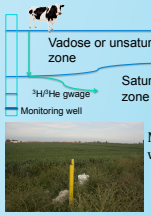

Monitoring well

To constrain vadose zone transit times, we sought to determine the penetration depth of dairy-derived nitrate in sediments underlying dairy farms, with the focus on the newest dairy (36-19). UC Davis sampled and archived drill core from monitoring wells installed as a part of a larger dairy groundwater project. Major anions (including nitrate and chloride) were extracted from sediment samples by leaching with water at LLNL. Anion concentrations were determined by ion chromatography (IC) at LLNL, and data are shown in this poster. Nitrate-oxygen and nitrate-nitrogen isotopic compositions will be determined with gas source isotope ratio mass spectrometry (IRMS) at LLNL.

Results

36-19

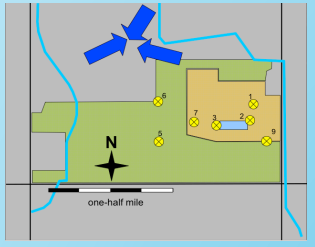

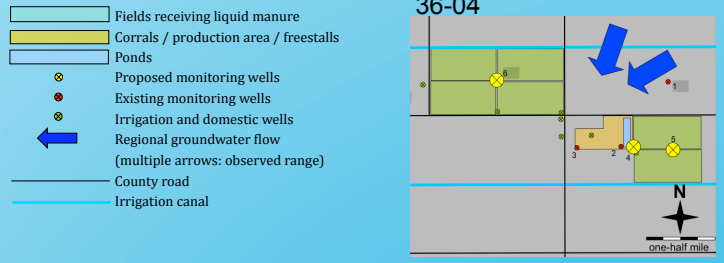

36-04

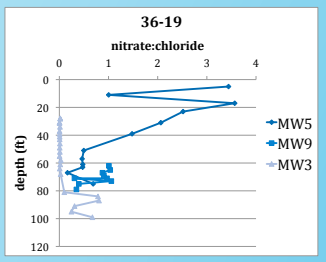

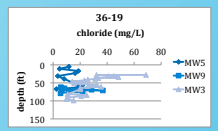

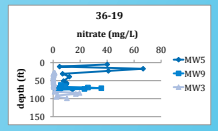

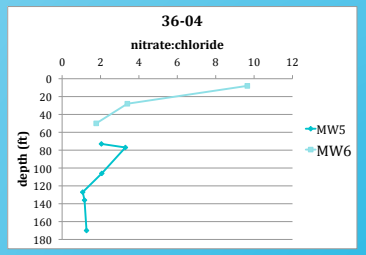

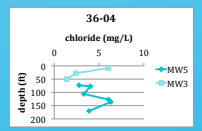

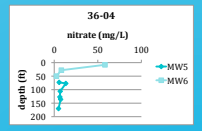

Discussion and Future Work

At both dairies, leachable soil nitrate and nitrate/chloride decreases with depth. The one exception is from a core adjacent to a dairy lagoon where wet soil N analyses show that ammonium is the dominant nitrogen species – in this core, nitrate is not detected in vadose zone. Given the large difference in the age of these dairies (5 years versus over 150 years), the data indicate that concentration profiles alone will not constrain nitrate transit time through the vadose zone without a transport model. Nitrate from the oxidation of ammonia in manure is generally enriched in the heavier 15N isotope when compared to soil nitrate (see figure). We are currently analyzing leachates for nitrate isotopic composition, and these data may provide stronger constraints on how deeply dairy-derived nitrate has penetrated the vadose zone in the five years that the 36-04 dairy has been in operation.

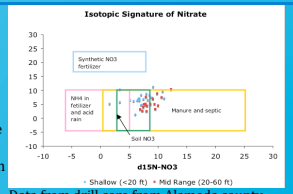

Data from drill core from Alameda county

This work performed under the auspices of the U.S. Department of Energy by Lawrence Livermore National Laboratory under Contract DE-AC52-07NA27344.

Post #

Extraction Chromatographic Studies of Db Homologs and Psuedo-Homologs

Megan E. Bennett[1], Roger A. Henderson[2], Dawn A. Shaughnessy[2]
1-Nuclear Forensics Internship
2- Lawrence Livermore National Laboratory, Physical and Life Sciences Directorate, Chemical Sciences Division
Glenn T. Seaborg Institute

Introduction

The goal of studying transactinide elements is to further understand the fundamental principles that govern the periodic table. The current periodic table arrangement allows for the prediction of the chemical behavior of elements. The correct position of a transactinide element can be assessed by investigating its chemical behavior and comparing it to that of the homologs and pseudo-homologs of a transactinide element. Homologs of a transactinide element are the elements in the same group of the periodic table as the transactinide. A pseudo-homolog of a transactinide element is an element with a similar main oxidation state and similar ionic radius to the transactinide element. For example, the homologs of Dubnium, Db, are Vanadium, Niobium and Tantalum (V, Nb and Ta); the pseudo homologs of Db are Protactinium, Pa, and Neptunium, Np. Understanding the chemical behavior of a transactinide element compared to its homologs and pseudo-homologs also allows for the assessment of the role of relativistic effects.

There are several challenges when studying the chemical behavior of transactinide elements. The first challenge is the low production rate of transactinides. Transactinides are produced on an atom-at-a-time basis, meaning that only one atom is ever available for chemical study. Because of this the chemical system being used must be selective for only one chemical state. The second challenge in transactinide chemistry is the short half-lives of the elements. Half-lives of the transactinides range from nanoseconds to a few hours. This leads to the need for fast chemistry. Another challenge is the need for a high degree of separation from interfering radionuclides so that the event with the transactinide element can be detected. Extraction chromatography lends itself very well to the needs of transactinide chemists because it provides rapid separation, high yields, large separation factors and requires only small volumes of solution.

Method

The goal of this project is study the chemical behavior of the lighter homologs and psuedo-homologs of Db on Eichrom's DGA Resin from HNO_3/HF and HCl/HF matrices. All samples were initially counted on a Ge gamma spectrometer for 30 minutes, evaporated to dryness and reconstituted in the desired matrix.

If the samples were to be used in column studies, they were loaded on to a vacuum box containing the DGA columns. If the samples were batch-wise, after re-constitution they were allowed to sit for 1hr then extracted into a clean centrifuge tube. After the desired experiment was performed the samples were then counted on the gamma spectrometer. These to counts allowed for the extraction or sorption behavior to be assessed.

^{95}Nb, ^{182}Ta, and ^{233}Pa were the radioisotopes used to assess the chemical behavior of this system. ^{95}Nb was obtained from the β decay of a ^{95}Zr source. ^{182}Ta was obtained from Isotope Products Laboratory and ^{233}Pa was obtained by the α decay of a ^{237}Np standard.

Results

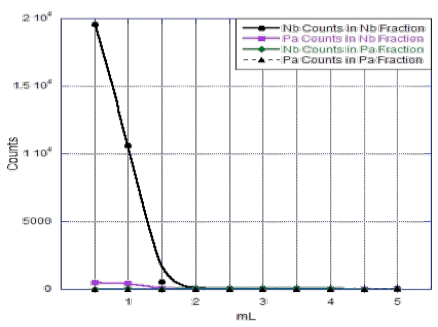

Figure 1. It was initially believed that Nb could be eluted separately from Pa by using 4M HNO_3 / 0.001M HF and 0.4M HNO_3 / 0.02M HF, respectively. The above elution curves show that both Nb and Pa elute off of DGA together in the Nb elution step.

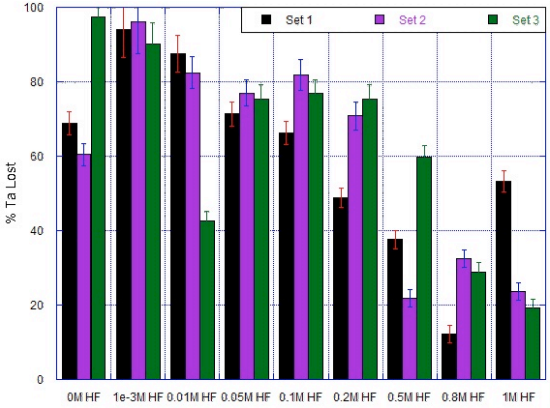

Figure 2. Ta is known to sorb to container walls. A variety of [HF] were studied while [HNO_3] was held constant at 4M. The larger variation within one set of conditions demonstrates that under these conditions the difficultly with ^{182}Ta is likely a mass issue due to additional Ta isotopes in the sample.

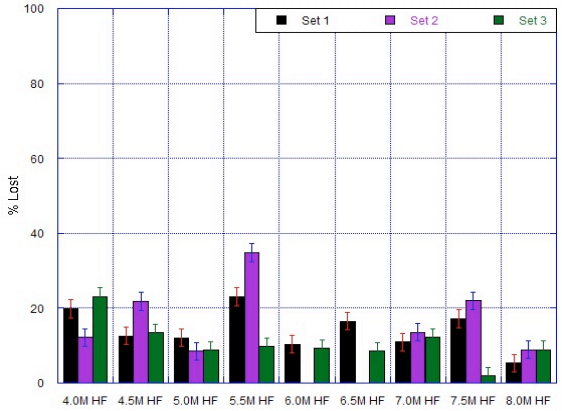

Figure 3. A Variety of [HF] were studied while [HCl] was held constant at 6M. When compared to Figure 2 it is evident that the mass issue in the ^{182}Ta solution is less problematic but still present.

Conclusion

Under current HNO_3/HF conditions Nb and Pa are inseparable on Eichrom's DGA resin. Further systematic studies varying both HNO_3/HF need to be done in order to separate Nb and Pa. The mass issue with loading ^{182}Ta from the reconstituted HNO_3/HF solution needs to be resolved before the behavior of Ta on Eichrom's DGA resin can be properly assessed. In order to do this carrier-free ^{182}Ta needs to be produced, this would be best done in accelerator based experiments. ^{182}Ta from the Isotope Product Laboratory loads more consistently from the HCl/HF system than from the HNO_3/HF system. Further column studies need to be investigated for loading Ta onto the DGA from the HCl/HF system, to ensure this different load solution will not effect the chemistry of the other Db homologs and psuedo-homologs.

This work performed under the auspices of the U.S. Department of Energy by Lawrence Livermore National Laboratory under Contract DE-AC52-07NA27344.

High Precision Uranium Isotope Measurement of Uranium Ore Concentrate: A Tool for Geolocation

Gregory A. Brennecka – Nuclear Forensics Internship Program
Lars E. Borg – Physical and Life Sciences

Glenn T. Seaborg Institute

Introduction and Goals: Uranium ore concentrate (UOC), a controlled nuclear material, is the final product of mining and milling operations worldwide. In cases of illicit trafficking, the chemical and isotopic signatures contained within UOC provide opportunity to trace the source of a sample of unknown origin. In this study, we examine the use of precise measurement of the $^{238}U/^{235}U$ and $^{235}U/^{234}U$ ratios for geolocation. Whereas it is unlikely that a single isotope system or measurement will produce an entirely unique isotopic signature for a uranium mine, the two uranium isotopic systems provide lines of evidence that can significantly narrow the field of possible source locations. Because the $^{238}U/^{235}U$ and $^{235}U/^{234}U$ have different fractionation mechanisms and vary independently, measurement of both ratios provides two independent "fingerprints" of the major component of UOC.

Methods: UOC samples from mines of various depositional environments were obtained and measured for $^{238}U/^{235}U$ and $^{235}U/^{234}U$ ratios to establish U isotope signatures. Results are shown in Figures 1 and 2 below.

The background image is a map of the major active and historic uranium mining districts of the world. Our goal is to have the capability to take an sample of unknown origin and source it to the original mine location.

^{234}U is a daughter product in the decay of ^{238}U. The damage caused in uranium bearing minerals by the α-recoil decay of ^{238}U to ^{234}U creates an environment susceptible to preferential leaching, creating excesses of ^{234}U in aqueous phases (groundwater). Interactions of each uranium deposit with modern groundwater are based on local geology. These interactions, coupled with the formation age of the deposit, create unique signatures in the proportion of ^{234}U relative to the other isotopes of uranium.

Figure 1a

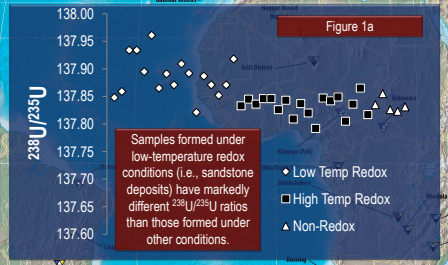

Samples formed under low-temperature redox conditions (i.e., sandstone deposits) have markedly different $^{238}U/^{235}U$ ratios than those formed under other conditions.

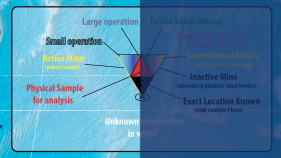

Error bars (2SD) are calculated based on multiple measurements of $^{238}U/^{235}U$ in CRM129A, a uranium isotope standard.

Figure 1

Error bars (2SD) are calculated based on multiple measurements of $^{235}U/^{234}U$ in CRM129A, a uranium isotope standard.

Figure 2

Conclusions: Using the various isotopes of uranium, it is possible to identify the potential source areas of an unknown sample of UOC. The $^{238}U/^{235}U$ provides information about the depositional environment in which the ore body was formed, specifically whether it formed in at low temperature. This can eliminate up to 2/3 of the potential source mines worldwide. In addition the $^{235}U/^{234}U$ provides a unique signature of interaction with modern groundwater. Thus, uranium isotope ratios, when paired with other lines of evidence in nuclear forensics provide essential predictive information that can be used to determe the provenance of an unknown sample.

Prepared by LLNL under Contract DE-AC52-07NA27344 LLNL Post - XXXXX

Estimating groundwater inflow to an alpine stream using Rn-222

Chris Cox – Nuclear Forensics Internship Program, University of Wyoming – Geology and Geophysics

Bradley K. Esser, Mike Singleton, Jean Moran (CalState), Richard Bibby – PLS/CSD

Glenn T. Seaborg Institute

University of Wyoming

Introduction

Background:
Climate change will potentially have a significant impact on alpine watersheds. It is predicted that increasing temperatures may result in a greater fraction of precipitation falling as rain, increase the frequency of rain on snow events, and change the timing and duration of spring snowmelt (IPCC). The degree to which groundwater may buffer the effects of these changes on river runoff is still poorly understood. This project attempts quantify the contribution of groundwater to surface stream flow.

Radon-222:
A product of the decay of U-238 (common in granitic rocks), Rn-222 concentrations in stream water can be used to estimate the amount of groundwater entering the stream. Our approach is similar to that used by Cook et al. (2008), however this study focuses on alpine streams with much different hydrogeologic regimes.

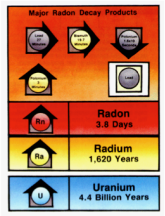

References:
Cook, P. G., Lamontagne, S., Berhane, D., and Clark, J. F., 2006. Quantifying groundwater discharge to Cockburn River, southeastern Australia, using dissolved gas tracers Rn-222 and SF6. *Water Resources Research* **42**, 12.
IPCC (Intergovernmental Panel on Climate Change): http://www.ipcc.ch

Field Site: Squaw Creek, Olympic Valley

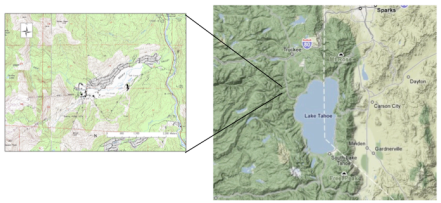

Olympic Valley is near lake Tahoe, and is home to Squaw Valley Ski Area.

Geology/Hydrology: The area is underlain by glacial till deposits consisting of Cretaceous Granite and Pliocene Volcanics. At least three north south trending Quaternary faults cross the study reach.

Field Work

Sample Collection/Methods: Both stream water and groundwater samples are analyzed for Rn-222. Because radon degases from water, care must be taken to minimize the amount of time the sample is exposed to the atmosphere after collection. For this reason, samples are collected by injecting 10mL of water beneath 20mL of a mineral oil scintillation cocktail. The scintillation vial is then sealed and any radon present will partition into the scintillation cocktail where it can be analyzed on an ultra low level liquid scintillation counter.

Results

Ground Water: Measured activities of Rn in groundwater sampled from wells is up to ten times the highest stream values.

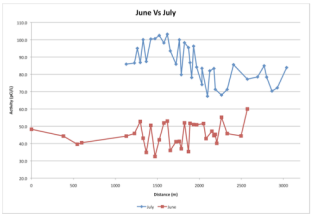

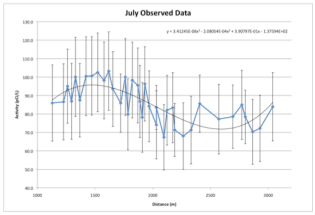

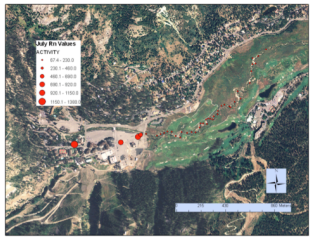

Stream: The measured Rn activities for each field work session are plotted as a function of distance downstream. Overall, Rn activities are higher in July and this is consistent with a stream that is receiving a greater percentage of flow from groundwater.

The high variability in the data may be due to analytical noise because the amount of error associated with each measurement effectively cancels out the small scale fluctuations. (See July Figure)

Modeling Rn-222

Theory:
A highly simplified model for Radon in stream water:

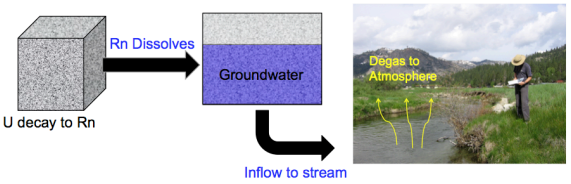

Mathematically this can be written as follows: (mass balance, steady state)

$$Q\frac{dc}{dx} = I(c_i - c) - kwc$$

Δ stream concentration = Input (groundwater inflow) – Output (degassing)

Numerical Solution:
The differential equation is solved using Euler's Forward Method. The amount of groundwater inflow (I) is then adjusted to best fit the observed data. In this way groundwater inflow can be estimated.

Preliminary Results:

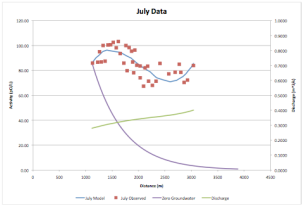

The observed values do not reflect a model with zero groundwater input (purple). This indicates that a significant percentage of stream flow is due to groundwater inflow. This is even more the case in July.

	Model Groundwater	% of flow
June	2.95 cfs	~6%
July	4.3 cfs	~45%

Conclusions:
While the quantity of groundwater generated by the model is reasonable, many of the model inputs need to be better constrained. Based upon downstream flow data, the amount of groundwater inflow modeled for July seems like an overestimate. This may be due to the current model being too simplistic. Future models will include components related to evaporation and water loss due to infiltration. Another important component is the interaction of the stream water with sediments in the streambed (hyporheic zone). Experiments are currently being performed to investigate how much stream Rn may be due to hyporheic zone sediments rather than groundwater influx.

Post #

This work performed under the auspices of the U.S. Department of Energy by Lawrence Livermore National Laboratory under Contract DE-AC52-07NA27344.

NanoSIMS Investigation of ^{36}Cl – ^{36}S Systematics in the Early Solar System

Benjamin Jacobsen[1] Jennifer Matzel[2] Ian. D. Hutcheon[2] Erick Ramon[2] Alexander N. Krot[3] Hope A. Ishii[2] Kazuhide Nagashima[3] Qing-zhu Yin[1]

[1]Department of Geology, University of California, Davis, CA 95616, USA (jacobsen@geology.ucdavis.edu). [2]Lawrence Livermore National Laboratory, Livermore, CA 94550, USA.
[3]Hawai'i Institute of Geophysics and Planetology, University of Hawai'i at Manoa, Honolulu, HI 96822, USA.

Glenn T. Seaborg Institute

Introduction

❖ The nucleosynthetic origin [c.f. 1-4] of short-lived radionuclides (SLR) has important implications for the use of SLR as high-resolution chronometers for dating early Solar System events.

- If SLR were produced by stellar sources, a homogeneous distribution of SLR is expected [e.g. 1,5].
- If SLR were produced by energetic particle irradiation near the proto-Sun, a heterogeneous distribution of SLR is expected [e.g. 3]. Together with ^{10}Be [6], ^{36}Cl is one of two SLR most likely produced by energetic particle irradiation within the Solar System [7-9].

❖ ^{36}Cl – ^{36}S system ($t_{1/2}$ ~0.3Ma) is a potential chronometer for dating of aqueous alteration in early Solar System materials.

❖ Previous ^{36}Cl-^{36}S studies of secondary sodalite in CAIs and chondrules by SIMS and NanoSIMS suggest $^{36}Cl/^{35}Cl$ varies between (>1.6-4)x10^{-6} [7,9-10]. This range may reflect:

- Temporal differences?
- Disturbances to the ^{36}Cl – ^{36}S system?
- Heterogeneous distribution of ^{36}Cl in the early Solar System?

❖ When did ^{36}Cl get incorporated into refractory CAIs?

❖ To further investigate and better constrain the abundance and distribution of ^{36}Cl in the early Solar System, we have studied the ^{36}Cl – ^{36}S systematics in wadalite, a Cl-rich ($Ca_6(Al,Si,Fe,Mg)_7O_{16}Cl_3$) secondary phase recently discovered in the Allende Type B CAI AJEF [11]

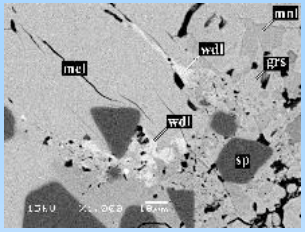

Figure 1. Backscattered electron image of wadalite (wdl) in AJEF. Wadalite occurs in secondary veins adjacent to melilite (mel) together with grossular (grs) and monticellite (mnl). Dark minerals are spinel (sp).

Sample

❖ The AJEF CAI has a well-constrained mineral and whole rock isochrons with $^{26}Al/^{27}Al$ ratio ~5x10^{-5} consistent the canonical value [12].

❖ Wadalite was initially characterized by electron microprobe and SEM, followed with Focused Ion Beam (FIB) sectioning and scanning transmission electron microscope (STEM) analyses [11].

❖ The wadalite in AJEF occurs adjacent to melilite in secondary veins associated with grossular, monticellite, and wollastonite (Fig. 1).

❖ Petrography suggests wadalite formation most likely involved interaction of grossular with Cl-rich fluids at modest temperature and pressure [11].

Experimental procedures

CIS isotope data were obtained using the Lawrence Livermore National Laboratory NanoSIMS in image rastering mode with a primary Cs^+ beam at ~8 pA and diameter of ~200 nm. Measurements were preformed in combined peak jumping, multi-collection mode, simultaneously measuring ^{28}Si, ^{32}S, ^{34}S and ^{36}S, and subsequently stepping the magnetic field to measure ^{37}Cl. A mass resolving power of ~3600 was used, sufficient to eliminate any contribution from $^{12}C_3^+$ or $^{35}ClH^-$; the intensity of the $^{35}Cl^{37}Cl^-$ dimer was estimated to be <0.01 sec^{-1}. Terrestrial wadalite with ~10x higher FeO than Allende wadalite showed no effects due to the doubly-charged interference , $^{56}Fe^{16}O^-$, on ^{36}S. Due to the low intensity of $^{36}S^-$, the background at mass 36 was carefully evaluated; the mean background intensity for wadalite, 0.002 sec^{-1}, is ~10x lower than for sodalite. No significant background correction was required for any wadalite data reported here. Measured $^{37}Cl^-/^{34}S^-$ ion ratios were converted to atomic ratios using a relative sensitivity factor of 0.71 ± 0.04, determined from measurements of terrestrial scapolite $(Na,Ca)_4(Al_3Si_9O_{24})Cl$. This relative sensitivity factor is similar to that reported by [10].

Magnesium-isotope compositions and $^{27}Al/^{24}Mg$ ratios of grossular in AJEF were measured *in situ* with the University of Hawai'i Cameca ims 1280 ion microprobe using a focused 57 µm primary ^{16}O ion beam. A primary current of 150 pA or 300 pA was used. Positively charged secondary ions were accelerated to +10 keV. The mass resolving power was set to ~3800, sufficient to separate interfering hydrides and doubly charged $^{48}Ca^{++}$. The relative sensitivity factors for aluminum and magnesium were determined from the $^{27}Al^+/^{24}Mg^+$ measured by SIMS and the Al/Mg ratios measured previously by electron microprobe for grossular.

Results

❖ The AJEF wadalite shows very large ^{36}S excesses ($\delta^{36}S$>209,500‰) correlated with the respective $^{35}Cl/^{34}S$ ratios (as high as 2,000,000). The slope of the best-fit line through the data yields an inferred $^{36}Cl/^{35}Cl$ ratio at the time of wadalite formation of (1.72□0.25)x10^{-5} (Fig. 2). This slope is ~410 times higher than the inferred $^{36}Cl/^{35}Cl$ ratio for the Pink Angel [7,10] and ~10x higher than that found for sodalite in Allende CAI #2 [13].

❖ Grossular adjacent to the wadalite, with $^{27}Al/^{24}Mg$ as high as ~100, shows no resolvable excess of ^{26}Mg. The inferred upper limited for the $^{26}Al/^{27}Al$ ratio in AJEF grossular is 9.1x10^{-7} (Fig. 3).

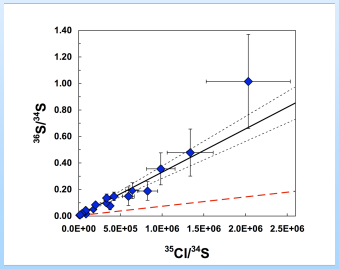

Figure 2. ^{36}Cl-^{36}S isotope correlation diagram of wadalite from Allende CAI AJEF. The black solid line is the best-fit regression through the data. The black dashed lines represent the error envelope. The uncertainties are 2σ. The red dashed line represents the inferred $^{36}Cl/^{35}Cl$ ratio for Pink Angel sodalite [7].

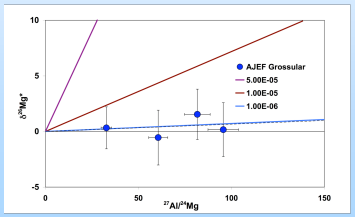

Figure 3. ^{26}Al-^{26}Mg isotope evolution diagram for grossular from Allende CAI AJEF. The uncertainties are 2σ. The black dashed line is the best-fit regression through the data of $^{26}Al/^{27}Al$ is ~ 9.1x10^{-7}.

Concluding remarks

❖ Solar energetic particle irradiation is the most likely source for ^{36}Cl production [1,7]. The $^{36}Cl/^{35}Cl$ ratio (~1.7x10^{-5}) determined from wadalite in AJEF is close to the value expected in a long-term irradiation scenario [8] and to the value predicted in the X-wind model of [14].

❖ As with sodalite in CAIs and chondrules, the Al-Mg isotope data for grossular in AJEF suggest ^{36}Cl in wadalite is decoupled from ^{26}Al. If the upper limit of the $^{26}Al/^{27}Al$ in grossular has any age significance the initial solar $^{36}Cl/^{35}Cl$ ratio could be as high as ~0.2.

❖ The use of ^{36}Cl as a chronometer for early solar system events has appeared infeasible due to the absence of any correlation between the inferred initial abundances of ^{36}Cl and ^{26}Al. However, if we assume the AJEF CAI started with ^{36}Cl levels as predicted by [8] for long term irradiation and the CAI formed in a X-wind scenario then our data suggests wadalite could have formed ~500,000 years after CAI formation.

References: [1] Wasserburg G.J. et al. (2006) *NPA*, 777, 5. [2] McKeegan K.D. & Davis A.M. (2007) *Meteorit., Comets Planets: Treatise on Geochem., ed. H. D. Holland & K. K. Turekian (Vol. 1)*, 431. [3] Shu F.H. et al. (2001) *ApJ* 548, 1029. [4] Gounelle M. et al. (2006) *ApJ* 640, 1163. [5] Boss, A.P (2007) *ApJ* 660, 1707. [6] McKeegan K.D. et al. (2000) *Science* 289, 1334. [7] Hsu W. et al. (2006) *ApJ*, 640, 525. [8] Leya I. et al. (2003) *ApJ* 594, 605. [9] Lin Y. et al. (2005) *Proc. Natl. Acad. Sci.*, 102, 1306. [10] Nakashima D. et al. (2008) *GCA* 72, 6141. [11] Ishii H. A. et al. (2008) *LPS XXXIX* Abst. #1989. [12] Jacobsen B. et al. (2008) *EPSL* 272, 353. [13] Ushikubo T. et al. (2007) *MAPS* 42, 1267. [14] Sahijpal S. and Soni P. (2006) *MAPS* 41, 953.

Work performed under the auspices of the DOE by LLNL under Contract DE-AC52-07NA27344, and an IGPP Minigrant to UC Davis.

Predicting the Activity Distribution of Nuclear Fallout

J.M. Klingsporn, Nuclear Forensics Internship Program
with K.B. Knight, G.D. Spriggs, C.L. Conrado, F.J. Ryerson, and I.D. Hutcheon

Glenn T. Seaborg Institute

NORTHWESTERN UNIVERSITY

Distribution and sources of activity from known nuclear events to validate nuclear fallout code predictions

How can we predict nuclear fallout in diverse environments?

It is important to be able to predict fallout activity distribution in any environment so we can:

- Rapidly understand extent of affected areas
- Determine the danger and dose rates to emergency workers
- Know where to recover optimal samples in order to gain additional information about the event

A computer code has been developed to provide better predictions of the distribution and activity of nuclear fallout:

- Based on the relationship between the size of grains drawn into the fireball and the activation of the grains and distribution of fallout.
- Due to surface area being inversely related to grain diameter the computer code predicts a 1/d relationship for fallout activity.
- Predicts the highest activity due to fallout is often found some distance from ground zero.

If the code is a reasonable approximation, then by knowing the distribution of grain sizes and the type of event, we can predict the activity distribution. *However, this code must be tested to establish its validity.*

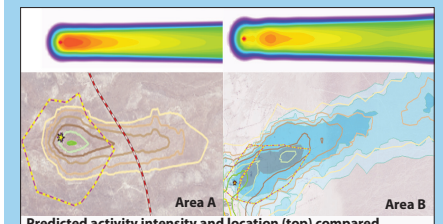

Predicted activity intensity and location (top) compared with data collected from an aerial survey (bottom)

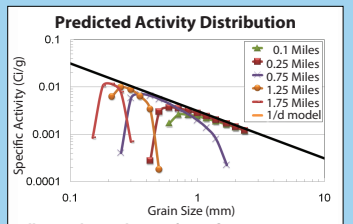

Fallout code simulation of specific activity 30 years after a one kiloton detonation in Area A

How are we testing the fallout code predictions?

To investigate the validity of the fallout code, we have:

- Collected soils from a known test along the plume of activity
- Separated the soils from each sample location by grain size
- Analyzed individual size fractions using gamma spectrometry
- Characterized the components of the bulk soil samples and their contributions to total measured activity

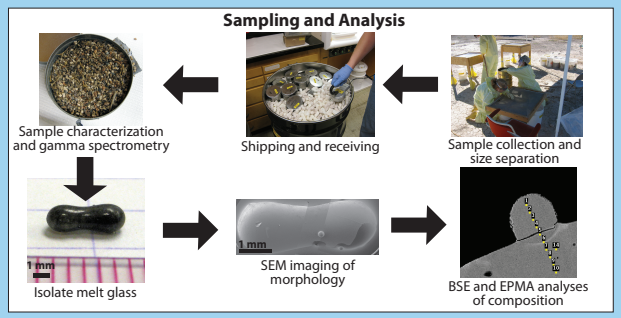

This work performed under the auspices of the U.S. Department of Energy by Lawrence Livermore National Laboratory under Contract DE-AC52-07NA27344

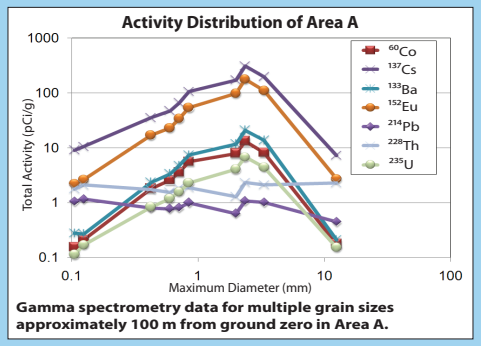

Gamma spectrometry data for multiple grain sizes approximately 100 m from ground zero in Area A.

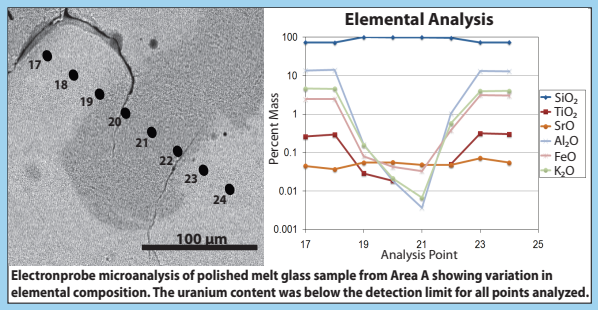

Electronprobe microanalysis of polished melt glass sample from Area A showing variation in elemental composition. The uranium content was below the detection limit for all points analyzed.

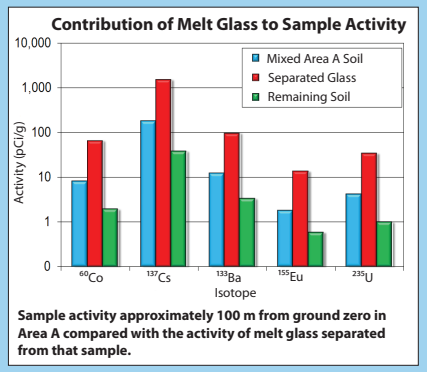

Sample activity approximately 100 m from ground zero in Area A compared with the activity of melt glass separated from that sample.

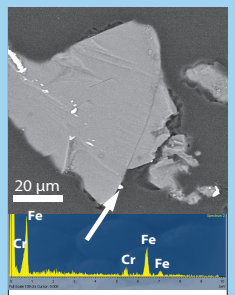

BSE image of unpolished grain from Area A showing iron and chromium adhered to grain surface.

How do we characterize and analyze these samples?

- All individual size fractions were analyzed using γ-spectrometry prior to shipping
- Select samples were re-analyzed in detail over five days using γ-spectrometry
- Melt glass was found and isolated from soil in select samples
- γ-spectrometry was performed on the glass and remaining soil separately, to characterize the contibution of each to total activity
- Secondary electron scanning electron microscopy was used to observe the range of sample morphologies and assess the mechanism of melt glass formation
- Backscattered electron microscopy was used to characterize sample composition, heterogeneity, and to identify sites of further interest
- Electron probe microanalysis (EPMA) quantified major and trace element compositions

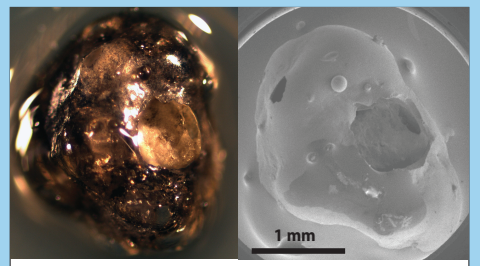

Optical and secondary electron images of a grain from Area A. Note that the grain has an outer coating of glass formed over a rocky core.

What have we learned?

- We can obtain relatively pristine soil samples after nearly five decades, which retain significant amounts of melt glass
- Grains act as nucleation sites and melt glass tends to condensate on these grains
- The data collected to this date follows the code predictions
- We need to analyze more samples with different grain size distributions to validate the fallout computer code

Where to go next?

- We are currently separating glass from multiple samples to study its contribution to the specific activity of the samples
- We are in the process of collecting other fallout soils with different grain size distributions to compare/confirm code predictions in more diverse conditions
- Once validated, codes such as this one may make it possible to rapidly predict the effects and activity distribution in the case of an urban nuclear event

LLNL-POST-415301

Origin, Chronology, and Evolution of Martian Basalts Deduced from the Study of Meteorite NWA 4468

Naomi Marks, Nuclear Forensics Internship Program
Lars E. Borg, Amy M. Gaffney, Chemical Sciences Division and Physical and Life Sciences Directorate

Glenn T. Seaborg Institute

UC DAVIS UNIVERSITY OF CALIFORNIA

THE DEPARTMENT OF GEOLOGY
UNIVERSITY OF CALIFORNIA, DAVIS

1. Introduction

Of the roughly 24,000 meteorites that have been discovered on Earth, only 38 or so have been identified as samples of the planet mars. As sample return from Mars remains a long way off, our best guess about the composition of the Martian crust and mantle comes from analyzing these meteorites that have fallen to Earth.

The martian meteorite suite contains a wide variety of rock types, including basalts and lherzolites (shergottites), clinopyroxenites (nakhlites), dunites (chassignites), and an orthopyroxenite. The most numerous of the martian meteorites are the shergottites, which exhibit a variety of mineralogies ranging from olivine-bearing primitive basalts and lherzolites (e.g. NWA1068 and NWA4468) to significantly more evolved pyroxene-plagioclase bearing basalts (e.g. Los Angeles and Shergotty). In addition to these mineralogical differences, the shergottites can be distinguished based on their trace element and isotopic compositions as well.

2. Relationship of NWA 4468 to other shergottites

To the right is a plot of present-day $^{87}Sr/^{86}Sr$-$\varepsilon^{143}Nd$ of shergottite source regions illustrating three distinct suites of samples. Triangles represent the oldest shergotites with strongly LREE depleted REE patterns. Squares represent shergottites with intermediate REE and Sr-Nd isotopic systematics. Circles represent the ~175Ma shergottites with the most enriched LREE patterns and sources with the most radiogenic Sr and least radiogenic Nd isotopic compositions. NWA4468 plots in the REE range of these most enriched patterns.

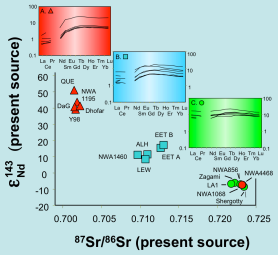

The compositional variability of the shergotites may be attributable to a combination of compositional heterogeneity in the martian mantle sources and variable degrees of fractional crystallization experienced by the mantle melts once leaving their source regions (Symes et al., 2009; Borg et al., 2005; Borg et al., 2003). Alternatively, the variability could be due to assimilation fractional crystallization (AFC) of differentiated crustal rocks (Jones, 1989).

We have begun Rb-Sr and Sm-Nd isotopic analyses on the primitive enriched olivine-bearing shergottite NWA 4468 in order to constrain the mechanisms responsible for the observed compositional diversity in the shergottite suite. By investigating how this relatively primitive and unfractionated meteorite obtained its enriched incompatible element signature, we hope to constrain the mechanism by which incompatible element variability is produced in the shergottite suite.

3. Petrology and Geochemistry

NWA 4468 is an olivine basaltic shergottite with ~35% olivine, ~35% clinopyroxene, ~25% maskelynite, and minor chromite, ilmenite, and phosphate. Bulk chemical analysis performed at LLNL by quadrupole ICP-MS for majors, minors, and trace elements with the exception of SiO_2. SiO_2 was measured by electron microprobe on bulk sample fused into a glass bead at UC Davis.

Table 1. Major and minor element composition (in wt%) for selected shergottites

	NWA4468	NWA1068	Zagami	NWA 856	Shergotty	Los Angeles
MgO	60.37	58.94	52.66	48.76	31.61	22.88
SiO_2	43.09	46.10	50.70	52.12	50.67	49.17
TiO_2	0.541	0.77	0.79	0.81	1.09	1.302
Al_2O_3	6.408	5.75	6.07	6.83	9.56	11.217
FeO	22.782	20.48	18.17	17.81	19.92	21.232
MnO	0.513	0.46	0.50	0.49	0.49	0.451
MgO	19.460	16.5	11.34	9.51	5.17	3.535
CaO	5.223	7.91	10.54	10.24	10.11	9.965
Na_2O	1.301	1.14	1.23	1.28	1.86	2.223
K_2O	0.146	0.16	0.14	0.13	0.24	0.240
P_2O_5	0.537	0.73	0.50	0.78	0.89	0.661
Total	100	100	100	100	100	100
Reference		Barrat 02	Lodders avg	Jambon 02	Stolper & McSween 79	Rubin 00

4. Sm-Nd and Rb-Sr Isotopic Analyses

Sm-Nd and Rb-Sr Isotopic Analyses

Preliminary Sm-Nd isotopic analyses on progressively leached whole rock samples yield an age of 150±29Ma and an initial εNd value of -6.9±0.3. The Sm-Nd tie line is interpreted to represent the crystallization age of the meteorite. The data from NWA4468 lie within error of the Sm-Nd isochron defined for NWA 1068 and suggest that these samples are closely related (Irving et al., 2007; Shih C.-Y. et al., 2003).

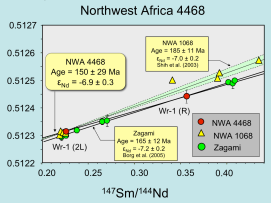

Although the Rb-Sr isotopic systematics of NWA4468 are disturbed as a result of terrestrial weathering, the leached mineral fractions typically lie on or near isochrons concordant with the Sm-Ndisochrons (Shih, C.-Y., 2003). The initial Sr isotopic composition is therefore estimated from the Rb-Sr isotopic systematics of the whole rock leach using the Sm-Nd age. This calculation yields a maximum initial $^{87}Sr/^{86}Sr$ ratio of 0.72258±14, a value in good agreement with the initial Sr isotopic composition of NWA1068 of 0.772230±3 calculated by Shih, C.-Y. (2003) (Borg et al., 2008).

5. Fractional Crystallization Models

The similarity of NWA4468 to other enriched shergottites and its fairly mafic major element composition suggested that shergottites such as NWA4468 and NWA1068 could be possibly be produced by assimilation and fractional crystallization processes. The MELTS algorithm (Ghiorso and Sack, 1995) is used to asses whether shergottittes could be produced by assimilation and fractional crystallization from a more magnesian parent.

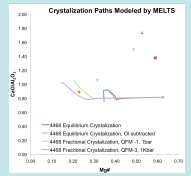

The liquid evolution paths for fractional and equilibrium crystallization models based on the MELTS algorithm (Ghiroso and Sack, 1995) indicate that NWA is a plausible parent composition for Los Angeles. The major element composition of Los Angeles can be produced by fractional crystallization of NWA4468. The major element composition of NWA1068 can be produced by equilibrium crystallization of NWA4468.

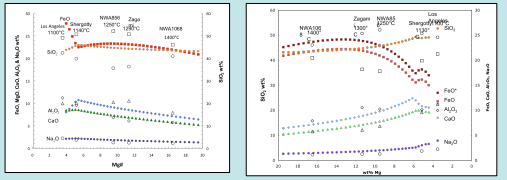

MgO wt% versus major element oxides of liquids calculated by MELTS assuming 1 bar pressure and starting material of NWA4468 at fO2 = QFM-1. Symbols represent 10°C steps starting above the liquidus temperature at 1600°C and continuing to 1100°C. Plot A assumes fractional crystallization of NWA4468, and the final liquid composition is a good match to the composition of Los Angeles. Plot B assumes equilibrium crystallization or olivine, clinopyroxene, feldspar, phosphates and spinel and indicates reasonable compositional matches to a number of enriched shergottites.

6. Future Work

Future work will include additional isotopic measurements based on mineral separates from NWA4468 and more detailed crystallization modeling, including modeling of REEs.

This work performed under the auspices of the U.S. Department of Energy by Lawrence Livermore National Laboratory under Contract DE-AC52-07NA27344.

Post #

LLNL-POST-415302

Cosmogenic ^{35}S Activity in Surface and Ground Water

Crystal Tulley (Master of Water Resources Program, University of New Mexico)
Bradley K. Esser, Richard Bibby, Everett Guthrie, Jean Moran & Sarah Roberts

Lawrence Livermore National Laboratory

THE UNIVERSITY of NEW MEXICO

Sulfur-35: A Natural Tracer in Water Resource Studies

Sulfur-35 is a cosmogenic radionuclide with great potential in groundwater recharge studies. It is a soft beta emitter with a half-life of 87 days that is produced in the upper atmosphere. Its presence in ground water indicates that some component of the groundwater recharged very recently (within months to a couple of years). Currently, the method is limited to low-sulfate waters in alpine basins. This project uses S-35 in an alpine basin setting and also develops the method for application to higher-sulfate water more typical of non-alpine settings.

Alpine Basin Field Site

Squaw Valley, NW of Lake Tahoe, is a sub-alpine basin that is expected to see significant changes in snow and as the climate warms. Samples were taken from Squaw Creek and from wells operated by the Squaw Valley Public Service Department, and were processed using the standard method.

Figure 1 Squaw Valley Site

Figure 2 California & Nevada Terrain Map

Photo 1 Part of Field Study Area

The Standard Method for Determination of Sulfur-35

In the standard method, a large volume (up to 20 L) of water sample is collected, sulfate is extracted onto anion exchange resin and then precipitated as barium sulfate, which is counted using Liquid Scintillation Counting. The method is calibrated for 100 mg of sulfate, and ion chromatography is used to determine sample sulfate concentration and necessary sample volume.

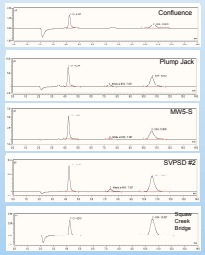

Figure 3 Ion Chromatographs

Name	Cl (mg/L)	NO_3 (mg/L)	SO_4 (mg/L)
Plump Jack	3.20 +/-0.01	0.96 +/-0.02	5.52 +/-0.03
MW5-S	11.35 +/-0.05	0.52 +/-0.00	15.92 +/-0.20
Confluence	0.83 +/-0.00	<0.16	0.80 +/-0.01
SVPSD #2	6.62 +/-0.00	1.84 +/-0.01	14.56 +/-0.20
Squaw Creek Bridge	1.20 +/-1.20	<0.16	4.50 +/-4.50

Based on the sulfate concentration, samples from Plump Jack, Confluence, and Squaw Creek Bridge require processing of 20 L, and MW5-S and SVPSD #2 require processing of 7 L for the Standard Batch Method.

The Modified Batch Method

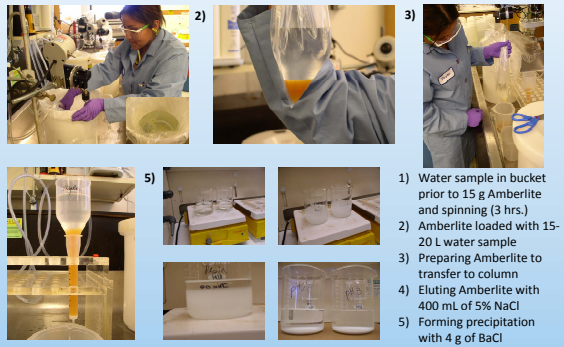

1) Water sample in bucket prior to 15 g Amberlite and spinning (3 hrs.)
2) Amberlite loaded with 15-20 L water sample
3) Preparing Amberlite to transfer to column
4) Eluting Amberlite with 400 mL of 5% NaCl
5) Forming precipitation with 4 g of BaCl

Limitations of the Standard Batch Method

Detection of ^{35}S is limited by the amount of water that can be collected and processed. The current batch method was developed to process100 mg of sulfate for determination of ^{35}S, and allows processing of 20 L of low-sulfate waters, including rain, snow, and alpine streams. Using this method, S-35 activity in typical rain and snow samples is 10-100 times above the detection limit.

Alpine streams and rainfall	0.2-5 mg/L
Lowland streams and rivers	10-100 mg/L
Polluted rivers and ground water	100-300 mg/L

Only small volumes of high-sulfate waters can be processed using the standard method, however, limiting detection of S-35 and the usefulness of the method for groundwater recharge studies in non-alpine basins. For example, only 2 L of a typical river water with 50 mg/L sulfate could be processed. Given the same absolute S-35 detection limit (as pCi), the volume-normalized detection limit (as pCi/L) for such a sample is an order of magnitude worse than achievable in a 20-L alpine stream water sample and may not be significantly above local rainfall activities.

Squaw Valley streams and ground waters are high in sulfate for an alpine basin (perhaps due to geothermal inputs along faults cutting the valley). While a snow sample had measureable S-35 activity (0.17 pCi/L) that was hydrologically reasonable (with an age of several months); ground waters and down-stream creek samples had high sulfate and undetectable sulfur-35

Developing a Method for High-Sulfate Waters

Two new or modified methods were developed to allow processing of high-sulfate waters: a modified batch method and a method using resin in place of barium sulfate.

Modified Batch Method

The goal of this method development was to increase sulfate loading from 100 mg to 1 g. This was accomplished by increasing the amount of Amberlite resin used (from 5 to 15 g), decreasing the pH of the load solution (to between 2 and 3), and increasing the NaCl concentration of the elute solution (from 3 to 5%). These changes produced only minimal degradation in counting efficiency and background, resulting in a detection limit almost an order of magnitude better than the standard batch method without adding complicated chemistry requiring additional lab ware or setup. Future work will involve processing natural water samples.

Background vs Mass Sulfate Analyzed

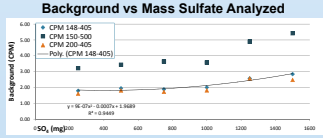

Efficiency vs Mass Sulfate Analyzed

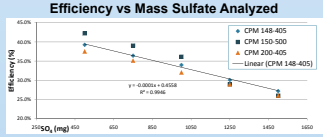

Detection Limits for Sulfur-35

	SO_4 (mg/L)	SO_4 (mg)	LLD (pCi/L)	LLD (pCi/g SO_4)
Alpine Rivers	0.2	4	0.0115	57.31
	5	100	0.0115	2.29
Lowland Rivers	10	200	0.0193	1.93
	50	1000	0.0254	0.51
	75	1500	0.0345	0.46

Analytical Parameters: 360-min count, 20 L sample, alpine rivers' efficiency & background determined empirically, 90% lowland rivers recovery.

Resin Method

The goal of the resin method was to concentrate sulfate onto a resin that could be suspended in an LSC cocktail to allow more sulfate to be loaded without significant quenching. TEVA-Spec resin from Eichrom has been used in this manner with technetium. We were not able to efficiently load sulfate onto TEVA-Spec in any of three trials where solution molarity, pH, and sulfate/resin ratios were varied. In future work, we will look at other resins.

This work performed under the auspices of the U.S. Department of Energy By Lawrence Livermore National Laboratory under Contract DE-AC52-07NA27344

Returning Summer Students at Work

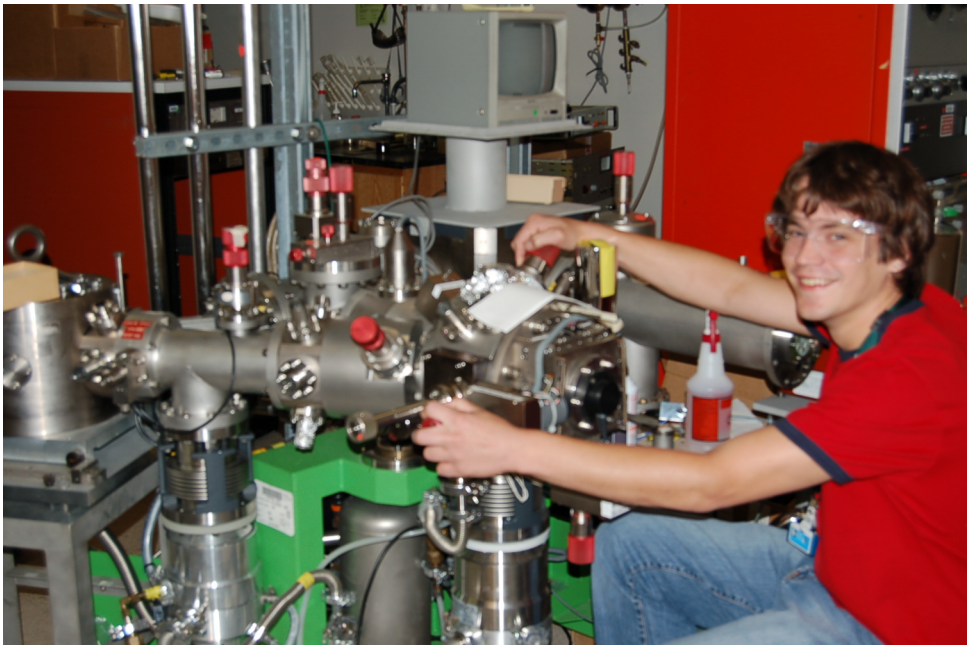

Disclaimer

Auspices

Lawrence Livermore National Laboratory is operated by Lawrence Livermore National Security, LLC, for the U.S. Department of Energy, National Nuclear Security Administration under Contract DE-AC52-07NA27344.